



1 **Exploring the Crucial Role of Atmospheric Carbonyl**
2 **Compounds in Regional Ozone heavy Pollution: Insights**
3 **from Intensive Field Observations and Observation-**
4 **based modelling in the Chengdu Plain Urban**
5 **Agglomeration, China**

6 Jiemeng Bao^{1,2}, Xin Zhang^{1,2}, Zhenhai Wu¹, Li Zhou³, Jun Qian⁴, Qinwen Tan⁵, Fumo
7 Yang³, Junhui Chen⁶, Yunfeng Li⁷, Hefan Liu⁵, Liqun Deng⁶, Hong Li^{1*}

8 ¹Chinese Research Academy of Environmental Sciences, State Key Laboratory of Environmental
9 Benchmarks and Risk Assessment, Beijing 100012, China

10 ²School of Environmental Science and Engineering of Peking University, State Key Joint Laboratory of
11 Environmental Simulation and Pollution Control, Joint Laboratory of Regional Pollution Control
12 International Cooperation of the Ministry of Education, Beijing 100871, China

13 ³College of Carbon Neutrality Future Technology, Sichuan University, Chengdu 610065, China

14 ⁴Sichuan Radiation Environment Management and Monitoring Central Station, Chengdu 611139, China

15 ⁵Chengdu Academy of Environmental Sciences, Chengdu 610046, China

16 ⁶Sichuan Academy of Eco-Environmental Sciences, Chengdu 610042, China

17 ⁷School of Mechanical Engineering, Beijing Institute of Petrochemical Technology, Beijing 102617,
18 China

19 Correspondence to: Hong Li (lihong@craes.org.cn)

20 **Abstract.** Gaseous carbonyl compounds serve as crucial precursors and intermediates
21 in atmospheric photochemical reactions, significantly contributing to ambient ozone
22 formation. To investigate the impact of gaseous carbonyls on regional ozone pollution,
23 simultaneous field observations and observation-based modelling of ambient carbonyls
24 were conducted at nine sites within the Chengdu Plain Urban Agglomeration (CPUA),
25 China during August 4-18, 2019, when three episodes of regional heavy ozone pollution
26 occurred across eight cities within CPUA. Throughout the study, the total mixing ratios
27 of 15 carbonyls ranged from 10.70 to 35.18 ppbv, in which formaldehyde (48.1%),
28 acetone (19.9%), and acetaldehyde (17.5%) were most abundant within the CPUA.
29 Ambient levels of carbonyls and ozone showed some positive correlations in space
30 (especially pronounced around Chengdu in both northern and southern directions) and



31 in diurnal variations with higher concentrations of carbonyls during ozone pollution
32 episodes. Photochemical reactivity analysis emphasized the significant contributions of
33 carbonyls, especially formaldehyde and acetaldehyde, to ozone formation. The ozone
34 formation sensitivity for sites experiencing severe ozone pollution were classified as
35 VOCs-limited regime, while others were categorized as transitional regime. Local
36 primary emissions, mutual air transportation among cities within the CPUA and
37 photochemical secondary processes were recognized to contribute significantly to the
38 production or the contamination of carbonyls in ambient air, with alkenes and alkanes
39 being important secondary precursors of carbonyls. This study highlights the pivotal
40 role of carbonyls in heavy ozone pollution within the CPUA, China, providing valuable
41 scientific insights to guide the development of effective countermeasures for regional
42 ozone pollution control in the future.

43 **Keywords:** Gaseous Carbonyls; Ozone Heavy Pollution; Pollution Characteristics;
44 Atmospheric Photochemical Reactivity; Source Analysis; The Chengdu Plain Urban
45 Agglomeration, China

46 1. Introduction

47 Atmospheric carbonyl compounds are pivotal in tropospheric chemistry, serving
48 as essential precursors to both ozone(O_3) and secondary organic aerosols(SOA) (Guo
49 et al., 2004). Over the past two decades, severe air pollution in China has driven
50 substantial research efforts to understand the contributions of carbonyl compounds to
51 these environmental challenges. Studies have shown that photolysis of carbonyl
52 compounds is a major source of RO_x radicals (Guenther et al., 2012; Y. Zhang et al.,
53 2016). These compounds can be photolyzed and react with OH radicals to form a large
54 number of HO_2 and RO_2 radicals, which increase the atmospheric oxidation capacity
55 and participate in the NO_x photochemical cycle, leading to ozone formation (Y. Zhang
56 et al., 2016; Meng et al., 2017). Additionally, dialdehydes such as glyoxal and
57 methylglyoxal undergo heterogeneous reactions with aqueous particulate matter,
58 rapidly forming SOA (Lou et al., 2010; Xue et al., 2016; Yuan et al., 2012). Ambient



59 carbonyl compounds not only affect the environment but also pose direct health risks
60 to humans. They can harm ecosystems through deposition and adsorption processes
61 (Yang et al., 2018). They also pose direct health risks to humans, including sensitization,
62 carcinogenesis, and mutagenicity (Fuchs et al., 2017).

63 Significant progress has been made globally in understanding the concentrations
64 (Xue et al., 2013; Duan et al., 2012), diurnal variations (Shen et al., 2013; Fu et al.,
65 2008), and sources of carbonyl compounds (Pang and Mu, 2006; Rao et al., 2016). The
66 results highlight the severity and spatial-temporal variations of carbonyl pollution in
67 China. The results highlight severe and spatiotemporal variations of carbonyl pollution
68 in China. High levels are found mainly in the North China Plain, the Yangtze River
69 Delta, and the Pearl River Delta (Duan et al., 2008; Shao et al., 2009; Tan et al., 2018;
70 Wang et al., 2018; Xue et al., 2014, 2013; Yang et al., 2017). Urban areas show higher
71 carbonyl levels than suburban and rural areas due to human activities (Xue et al.,
72 2013). Despite many studies focusing on urban areas in China and comparing carbonyl
73 compound concentrations across different regions, there is a lack of comprehensive
74 analysis of atmospheric carbonyl compounds over larger areas, such as urban
75 agglomerations. In addition, most ground observations have been concentrated in fast-
76 developing regions, such as the NCP, YRD, and PRD. Existing research often
77 emphasizes overall VOCs rather than specific carbonyl compounds and their roles in
78 ozone pollution, leading to an incomplete understanding of the mechanisms by which
79 carbonyl compounds contribute to ozone formation and their regional differences.

80 Monitoring carbonyl compounds in the atmosphere is challenging due to their
81 typically low concentrations (ppt-ppb levels), necessitating highly sensitive analytical
82 methods. The diversity of carbonyl compounds, including multiple isomers, requires
83 highly selective analytical techniques for differentiation. Current measurement
84 technologies limit our understanding of the spatiotemporal distribution of carbonyl
85 compounds, affecting the accurate assessment of their environmental behavior, sources,
86 and transport. While previous studies have recognized the importance of carbonyl



87 compounds in ozone formation, detailed evaluations of their specific roles remain
88 insufficient.

89 Atmospheric carbonyl compounds originate from both primary and secondary
90 sources. Primary sources include the incomplete combustion of fossil fuels and biomass,
91 industrial emissions, emissions from the catering industry, and releases from plants.
92 Secondary sources arise from the atmospheric photochemical oxidation of VOCs
93 (Xue et al., 2013), particularly alkenes, aromatics, and isoprene, which typically
94 dominate the secondary formation of carbonyls. Existing source apportionment
95 methods, such as characteristic species ratio, source tracer proportion, multiple linear
96 regression, parameterization method based on photochemical age, and acceptor model,
97 struggle to distinguish between primary sources and secondary formation accurately.
98 The emission patterns of primary sources, particularly non-vehicle sources, are not well
99 understood. The source apportionment results elucidate the necessity to
100 comprehensively understand the secondary formation mechanisms of carbonyls.
101 Despite advancements in the study of atmospheric carbonyl compounds, significant
102 gaps remain in understanding their spatiotemporal distribution, source apportionment,
103 and contribution to ozone pollution. These gaps limit our comprehensive understanding
104 of the behavior of carbonyl compounds in the atmosphere, particularly in specific
105 regions and larger areas.

106 In this context, this study focuses on atmospheric carbonyl compounds and their
107 roles in photochemical pollution within the Chengdu Plain Urban Agglomeration
108 (CPUA) of China. The CPUA includes eight cities: Chengdu, Mianyang, Deyang,
109 Leshan, Meishan, Yaan, Suining, and Ziyang. This region has a developed economy
110 and a high degree of internationalization. The CPUA is located on the western edge of
111 the Sichuan Basin, surrounded by mountain ranges, which easily block airflow. The
112 unique climatic environment of the CPUA features low wind speeds year-round, high
113 frequency of static winds, short hours of sunshine, frequent winter inversions, and a
114 pronounced heat island effect in summer. These climatic characteristics significantly



115 impact the variations in air pollutant concentrations, making the region prone to ozone
116 pollution in summer and haze pollution in winter. (Li et al., 2013; Hu et al., 2017; Zhang
117 et al., 2010). Although previous studies have shown that ozone formation in urban
118 Chengdu is primarily VOCs-limited (Tan et al., 2018), with aromatic hydrocarbons and
119 alkenes contributing significantly to ozone generation in summer (Xu et al., 2020),
120 these studies mainly focus on single cities and overall VOCs. There is limited
121 understanding of the distribution, sources, and specific roles of carbonyl compounds
122 across the entire CPUA and their contributions to regional ozone pollution and mutual
123 air transport mechanisms.

124 To address these research gaps, this study involves an intensive field observation
125 experiment conducted by the Sichuan Academy of Environmental Sciences, Peking
126 University, Sichuan University and Chinese Academy of Environmental Sciences.
127 Atmospheric carbonyl compounds were observed at nine sites in eight cities within the
128 CPUA for 15 days during a period of heavy ozone pollution in August 2019. Samples
129 were analyzed using 2,4-dinitrophenylhydrazine solid phase adsorption/high
130 performance liquid chromatography (HPLC). The study aims to characterize the
131 atmospheric carbonyl compounds in the CPUA, assess their influence on
132 photochemical pollution, identify key carbonyl compounds that may play crucial roles
133 in heavy ozone pollution in the CPUA, and evaluate the contribution of primary
134 emissions, air pollution transport, and secondary generation to key carbonyl compounds
135 through a combination of multivariate linear regression modeling and OBM. This
136 research aims to provide technical support for controlling carbonyl compounds
137 pollution in the CPUA and to reduce their contributions to ozone pollution.

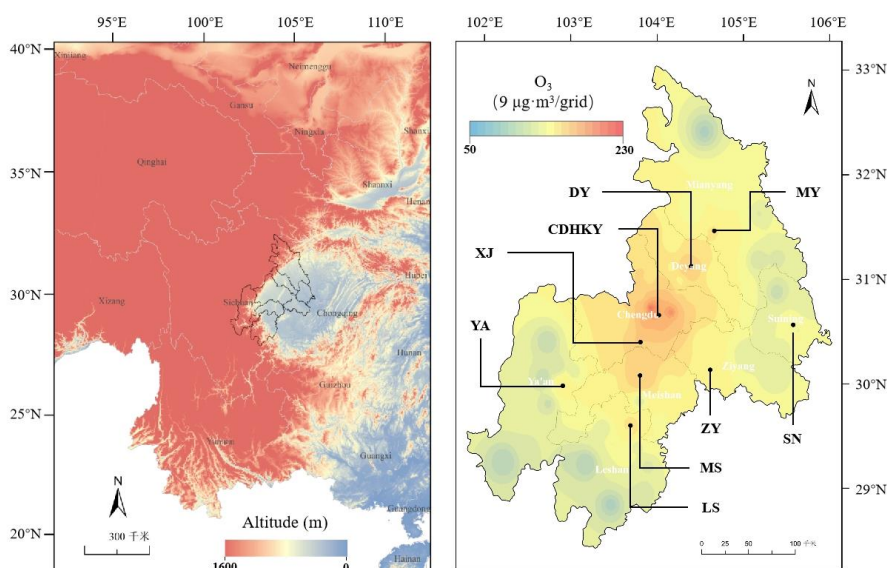
138 **2. Materials and methods**

139 **2.1 Observation Sites Profile**

140 In this study, a total of 9 off-line sampling sites for atmospheric carbonyl
141 compounds were set up in 8 cities in the CPUA from August 4th to 18th, 2019(table S1).



142 Considering that this study focused on the pollution characterization of carbonyl
143 compounds in urban areas, one urban site was selected in each city. In addition, in order
144 to compare and study the pollution characteristics of carbonyl compounds in the
145 suburbs, a suburban site was set up in XJ County, Chengdu City. For the selection of
146 urban sites in each city, priority is given to those choices of set-up in the vicinity of the
147 state-controlled site, and the perimeter of the sites should be open, unobstructed and no
148 obvious pollution sources, with convenient transportation and power supply. The
149 distribution of specific sites is shown in Fig. 1.



150

151

Figure 1. Sampling sites distribution.

152 2.2 Samples Collection

153 The sampling of atmospheric carbonyl compounds mainly referred to the TO-11A
154 standard of the United States Environmental Protection Agency (US EPA) and the
155 Chinese environmental protection standard HJ 683-2014 High Performance Liquid
156 Chromatography Method for the Determination of Atmospheric Carbonyl Compounds,
157 and the sampling was carried out by using silica gel sampling tubes (IC-DN3501 from
158 Tianjin Bonna-Agela) coated with DNPH (2,4-dinitrophenylhydrazine). In this study,
159 an automatic sampler for carbonyl compounds (Zhang et al., 2019) was used to



160 continuously collect atmospheric carbonyl compounds. From August 4th to 18th, 2019,
161 air samples were collected every 2 hours with a sampling flow rate of 0.8 L/min. In
162 addition, in order to prevent the impact of ozone and rainwater in the atmospheric air
163 on sample collection, a potassium iodide ozone removal column (KI 140 from Tianjin
164 Bonna-Agela) was installed and a water removal agent made by ourselves (Bao et al.,
165 2022; Wang et al., 2020) was added at the front end of the sample tube. Two blank
166 samples were collected before and after the sampling, and blank samples were also
167 collected for different batches of sampling tubes. The samples were frozen at -18°C and
168 analyzed within one month.

169 Atmospheric VOCs were sampled using SUMMA tanks, stainless steel tanks with
170 electropolished and silanized inner walls, manufactured by Entech in the United States,
171 with a sampling volume of 3.2 liters. The sampling was controlled by a constant current
172 integral sampler to sampling for an average of 1 hour. The sampling time was from
173 August 4th to 18th, 2019, and 2 VOCs samples were collected per day at each site (not
174 collected under special weather conditions such as rain), and each sample was collected
175 for 1 hour controlled by a cross-flow integration sampler. One sample was collected
176 from 8:00 to 9:00, and one sample was collected from 14:00 to 15:00, of which 6
177 samples were collected per day on August 11th, 12th and 16th (8:00-9:00, 10:00-1:00,
178 12:00-13:00, 14:00-15:00, 16:00-17:00, and 18:00-19:00).

179 2.3 Samples Analysis

180 The carbonyl compounds samples were qualitatively and quantitatively analyzed
181 by using High Performance Liquid Chromatography (HPLC) (LC-20AD, Shimadzu,
182 Japan) and an ultraviolet detector (SPD-20A, Shimadzu, Japan), mainly based on the
183 US EPA TO-11A standard and the Chinese HJ 683-2014 standard. The DNPH sampling
184 column after sampling was slowly eluted into a volumetric flask using acetonitrile
185 (chromatographically pure, Thermo Fisher Scientific China) to 5.0 mL. Then 1.5 mL
186 sample was taken into an HPLC sample bottle, and sealed and stored in a refrigerator
187 at <4 °C to complete the pre-treatment. Prior to sample analysis, a standard solution of



188 the concentration gradient was prepared using TO-11A standard solution (Supelco,
189 USA) and used as the external standard. The correlation coefficient (R^2) of the standard
190 curve was greater than 0.995. The limit of detection of the device was 0.56~5.57 ng/mL,
191 and the limit of quantification was 1.87~18.56 ng/mL (Table S2). Then 20 μ L of the
192 pretreated sample was extracted through the autosampler and injected into the
193 HPLC/UV system, detected by a UV detector with a wavelength of 360 nm, qualified
194 by retention time value, quantified by peak area value, and the qualitative and
195 quantitative analysis data of carbonyl compounds were obtained after conversion. The
196 HPLC conditions referred to Chinese environmental protection standard HJ 683-2014:
197 binary gradient washing was performed using acetonitrile and water, 60% acetonitrile
198 was held for 20 mins, acetonitrile was increased linearly from 60% to 100% within 20-
199 30 mins, and acetonitrile was reduced to 60% again within 30-32 mins and held for 8
200 mins; the column oven was kept at 40 °C.

201 The atmospheric VOCs were analyzed using the TO-14 and TO-15 methods
202 recommended by the US EPA, that is, frozen preconcentration coupled with gas
203 chromatography and mass chromatography. The sample was pre-concentrated by
204 Entech7100 system at a low temperature, then the VOCs components were quantified
205 by Agilent gas chromatography coupled with mass spectrometry instrument (GC-MS).
206 The concentrated samples were separated by gas chromatography and then entered
207 mass spectrometry for detection. A hydrogen flame ionization detector (FID) was used
208 to detect 5 substances: ethane, ethylene, acetylene, propane, and propylene. During the
209 sample analysis, four internal standard gases bromochloromethane, 1,4-
210 difluorobenzene, chlorobenzene-d5 and 4-bromofluorobenzene were used. With a
211 standard gas containing 118 substances such as PAMS, TO-15 and carbonyl compounds,
212 a multi-point calibration standard working curve was established using 6 concentration
213 gradients.

214 2.4 Data Analysis

215 2.4.1 Ambient levels comparison



216 According to the Technical Regulation on Ambient Air Quality Index (on trial),
217 National Environmental Protection Standard of the People's Republic of China HJ
218 633—2012, days with an ozone pollution index (IAQI) of 100 or higher during the
219 observation period were designated as pollution days, while days with an IAQI below
220 100 were considered clean days. This study compared the pollution characteristics of
221 carbonyl compounds between pollution days and clean days. Additionally, the
222 concentrations of formaldehyde, acetaldehyde, and acetone observed during the
223 summer of 2009-2013 in economically developed and industrialized areas such as
224 Beijing, Shanghai, and Guangzhou in China, as well as locations in South America
225 (Brazil), Asia (Thailand), Europe (France), and North America (United States), were
226 selected and compared.

227 **2.4.2 Ozone formation sensitivity inferring**

228 Previous studies have shown that the formaldehyde to NO₂ ratio (FNR) can be
229 used to determine the sensitivity of O₃-NO_x-VOCs (Schroeder et al., 2017; Tonnesen
230 and Dennis, 2000; Vermeuel et al., 2019). Most studies used satellite remote sensing-
231 based FNR, but the FNR column concentration ratios inverted by satellite remote
232 sensing mainly represented the average photochemical of the troposphere, and the
233 concentration distributions of HCHO and NO₂ in the vertical direction were
234 inconsistent (Hong et al., 2022; Schroeder et al., 2017). So, there is a large uncertainty
235 to develop ground-level ozone pollution prevention and control measures. In this study,
236 sensitivity analysis of ground-level ozone formation was carried out based on the ratio
237 of ground-level HCHO to NO₂ during the observation period at the 9 sites of 8 cities in
238 the CPUA. $FNR < 0.55 \pm 0.16$ and $FNR > 1.0 \pm 0.3$ were defined to VOCs-limited and
239 NO_x-limited, respectively, and FNR ratio ranged from 0.55 ± 0.16 to 1.0 ± 0.3 defined to
240 NO_x and VOCs co-limited (Liu et al., 2021; Zhang et al., 2022).

241 **2.4.3 Secondary formation mechanism investigation**



242 **(1) Atmospheric chemical reactivity**

243 In this study, the contribution of atmospheric chemical reactivity of carbonyl
244 compounds to ozone formation was evaluated using the OH free radical consumption
245 rate (L_{OH}) and ozone formation potential (OFP):

$$246 L_{OH} = [\text{OVOC}]_i \times K_i(\text{OH}) \quad (1)$$

247 Where, $[\text{OVOC}]_i$ was the observed concentration of the i^{th} ($i=1$ to n) carbonyl
248 compound, in molecule/cm³; $K_i(\text{OH})$ was the rate constants of the i^{th} carbonyl
249 compound reacting with OH radicals, in cm³/(molecule·s); the selected $K_i(\text{OH})$ values
250 were from literature (Atkinson and Arey, 2003).

$$251 \text{OFP} = \text{MIR}_i \times [\text{OVOC}]_i \quad (2)$$

252 Where, MIR was the maximum incremental reactivity of the i^{th} carbonyl
253 compound, and the MIR values of each species were from California Code of
254 Regulations (<https://govt.westlaw.com>); $[\text{OVOC}]_i$ was the mass concentration of the i^{th}
255 carbonyl compound, in µg/m³.

256 **(2) Observation-based model (OBM)**

257 The relative incremental activity (RIR) was calculated by assuming that the
258 concentration of a given carbonyl compound precursor decreased by a certain
259 proportion could cause the change of the concentration of the carbonyl compound, so
260 as to further judge the effect of VOCs on the formation of carbonyl compounds.
261 Combining the concentrations and activity levels of 15 carbonyl compounds during the
262 observation period, this study focused on formaldehyde, acetaldehyde, and acetone as
263 the primary research targets. The impacts of various AVOCs (anthropogenic VOCs),
264 including alkanes, alkenes, alkynes, and aromatic hydrocarbons, as well as BVOCs
265 (biogenic VOCs) like isoprene, on the formation of formaldehyde, acetaldehyde,
266 and acetone were assessed using observation-based OBM classification. Specific
267 species of anthropogenic source VOCs (alkanes, alkenes, alkynes, and aromatic
268 hydrocarbons) and biogenic VOCs (isoprene) are detailed in Table S3.



269 VOCs observations, conventional gases (NO₂, CO and SO₂) and meteorological
270 parameters (temperature, relative humidity and pressure) were imputed into the model.
271 It was assumed that the pollutants are well mixed. Under the constraints of the measured
272 hourly concentration data of pollutants, the atmospheric chemical process was
273 simulated to obtain the source-effect relationship of the measured pollutants. By
274 assuming the reduction of the source effect, the RIRs of different carbonyl compounds
275 precursors were calculated, and the sensitivities of carbonyl compounds to different
276 pollutants were obtained, and then the secondary formation mechanism of carbonyl
277 compounds was determined. The formula to calculate the RIR is as follows:

$$278 \quad RIR(X) = \left[\frac{\Delta P_Y(X)/P_Y(X)}{\Delta S(X)/S(X)} \right] \quad (3)$$

$$279 \quad P_Y = Y_{\text{net formation}} - Y_{\text{net consumption}} \quad (4)$$

280 Where X was a specific species; P_Y(X) was the net formation rate of species y;
281 S(X) was the total amount of emissions of species X in a certain period, i.e., the source
282 effect of species X. ΔS(X) was the change in total emissions of X caused by the
283 hypothetical change in source effect, ΔP_Y(X) was the change in P_Y(X) after the change
284 in source effect S(X), and RIR(X) was the relative incremental reactivity of species X.
285 The species Y in this study were formaldehyde, acetaldehyde and acetone, respectively,
286 and pollutant X was reduced by 20%.

287 The absolute RIR of the precursor reflects the sensitivity of carbonyl compounds
288 formation to the precursor. The higher the absolute RIR, the more sensitive the carbonyl
289 compounds formation to the precursor. A positive RIR value indicates that reducing the
290 species can reduce the formation rate of species Y, and a negative RIR value indicates
291 that reducing the species can increase the formation rate of species Y.

292 2.4.4 Sources Analysis

293 (1) Multi-linear regression model

294 There is a good correlation between concentrations of compounds of the same or



295 similar source in the atmosphere. Based on this property, it was assumed that the
296 primary and secondary sources of carbonyl compounds were linearly correlated with
297 the selected tracers, and then a quantitative source model was established by multiple
298 linear statistical regression analysis (Kanjanasiranont et al., 2016a; Li et al., 2010; Ling
299 et al., 2017; Luecken et al., 2012; Lui et al., 2017; Wang et al., 2017). In general, CO is
300 the marker product of typical anthropogenic combustion source emissions, mainly from
301 vehicle exhaust emissions and coal combustion. Ozone, as an indicator of
302 photochemical smog, is a typical secondary formation pollutant. In this study, CO and
303 ozone were selected as the tracers of primary source and secondary source of carbonyl
304 compounds, respectively. The formula is as follows:

$$305 \quad [carbonyl] = \beta_0 + \beta_1[CO] + \beta_2[O_3] \quad (6)$$

306 Where [carbonyl], [CO] and [O₃] represented the observed mixing ratios of
307 carbonyl compounds, CO and ozone, respectively, in ppbv. β_0 , β_1 and β_2 were
308 coefficients obtained by multiple linear regression fitting model, in ppbv/ppbv. β_0
309 represented the background concentration of a given carbonyl compound, β_1
310 represented the emission ratio of the carbonyl compound relative to CO. $\beta_1[CO]$ and
311 $\beta_2[O_3]$ represented the concentrations of carbonyl compound in primary emission and
312 secondary formation, respectively, in ppbv.

313 In addition, the relative contribution of primary emissions, secondary formation
314 and background concentrations of carbonyl compounds can be calculated using the
315 following formula:

$$316 \quad P_{primary} = \frac{\beta_1[CO]_i}{(\beta_0 + \beta_1[CO]_i + \beta_2[O_3]_i)} \times 100\% \quad (7)$$

$$317 \quad P_{secondary} = \frac{\beta_2[O_3]_i}{(\beta_0 + \beta_1[CO]_i + \beta_2[O_3]_i)} \times 100\% \quad (8)$$

$$318 \quad P_{background} = \frac{\beta_0}{(\beta_0 + \beta_1[CO]_i + \beta_2[O_3]_i)} \times 100\% \quad (9)$$

319 Where, $P_{primary}$ represented the contribution of the primary emission of a given
320 carbonyl compound, %; $P_{secondary}$ represented the contribution of the secondary
321 formation of the carbonyl compound species, %; $P_{background}$ represented the contribution



322 of the carbonyl compounds species from sources other than primary emissions and
323 secondary formation, %.

324 (2) Backward trajectory model

325 The effects of long-distance air mass transport on the pollution of carbonyl
326 compounds in the CPUA were studied using MeteoInfo software and TrajStat plug-in.
327 In this model, meteorological data were relevant meteorological data from the global
328 date assimilation system (GDAS) database
329 (<ftp://arlftp.arlhq.noaa.gov/pub/archives/gdas/>). A trajectory simulation height of 500
330 m was selected. The duration of backward trajectory was 48 h. The daily start time was
331 00:00 UTC. The analog frequency was 2 h. The backward trajectory diagram was
332 calculated. Meanwhile, the clustering method in TrajStat software and the Euclidean
333 distance algorithm were used to cluster the airflow trajectory to the CPUA. And then
334 the statistical analysis was carried out in combination with the corresponding pollutant
335 mass concentration characteristics.

336 3. Results and Discussion

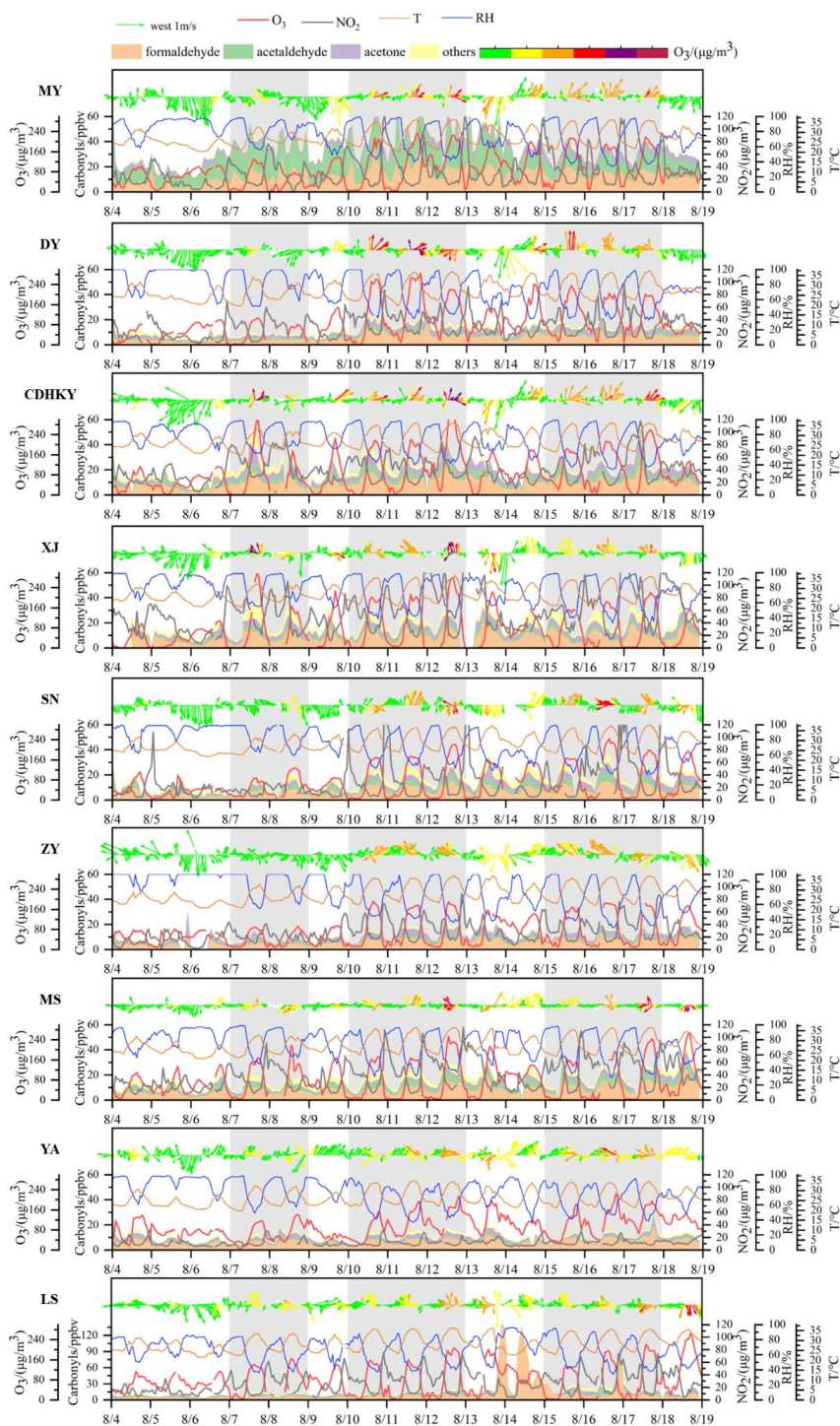
337 3.1 Overview of air quality during observation period

338 Due to the influence of cooling and precipitation caused by cold air intrusion, the
339 early observation period (from August 4th to 6th, 2019) in the Chengdu Plain Urban
340 Agglomeration (CPUA) experienced slightly lower temperatures (25.1°C) and higher
341 humidity (87.6%). These conditions were not conducive to ozone formation. However,
342 as temperatures rose and humidity decreased thereafter, favorable conditions for ozone
343 generation emerged, leading to heavy and persistent regional ozone pollution in the
344 CPUA. By August 12th, the mean temperature had gradually increased to 29.1°C, while
345 it averaged 27.7°C from August 13th to 14th. During this time, cumulative precipitation
346 reached 975 mm, resulting in temporary alleviation of ozone pollution. Subsequently,
347 temperatures rose again from August 15th to 18th, with the mean temperature persisting



348 above 28.4°C for several days, accompanied by a decrease in humidity to a minimum
349 of 64.8% on August 17th. Overall, during the observation period (from August 4th, 2019,
350 0:00 to August 18th, 2019, 24:00), three episodes of severe ozone pollution occurred,
351 namely EP1 (August 7th to 9th), EP2 (August 10th to 13th), and EP3 (August 15th to 18th),
352 as depicted in Fig. 2.

353 Fig.3 illustrates the temporal and spatial variations of ozone and NO₂
354 concentrations, as well as temperature and humidity at each site during the observation
355 period. After observing the spatial distribution of ozone concentration during EP1, it's
356 evident that the severity of pollution reached heavily polluted levels, with Chengdu
357 recording an O₃-8h concentration of 297 µg/m³ on August 7th. This distribution
358 demonstrated a radial decrease from Chengdu to the surrounding areas. However, the
359 subsequent episodes, EP2 and EP3, exhibited even broader ranges of ozone pollution
360 and more pronounced spatial movements. During the early stages of EP2 and EP3 (from
361 August 10th to 11th and from August 14th to 15th, respectively), high ozone
362 concentrations were observed in the Chengdu-Deyang-Mianyang region. In the middle
363 stages (August 12th and from August 16th to 17th, respectively), influenced by northerly
364 airflow, regions with high ozone concentrations expanded to the central (Meishan,
365 Ziyang, and Suining) and southwestern (Leshan and Ya'an) parts of the CPUA. In the
366 later stages (August 13th and August 18th), under the influence of northwesterly airflow,
367 regions with high ozone concentrations (Meishan and Leshan) moved southward again,
368 while ozone pollution in other areas of the CPUA gradually weakened. On August 11th
369 to 12th and August 16th to 17th, ozone concentrations in the eight cities of the CPUA
370 reached light pollution levels or higher, with the heaviest pollution recorded on August
371 12th. Specifically, Deyang, Mianyang, Suining, and Meishan reached moderate
372 pollution levels, while Chengdu reached heavy pollution with a concentration of 324
373 µg/m³.



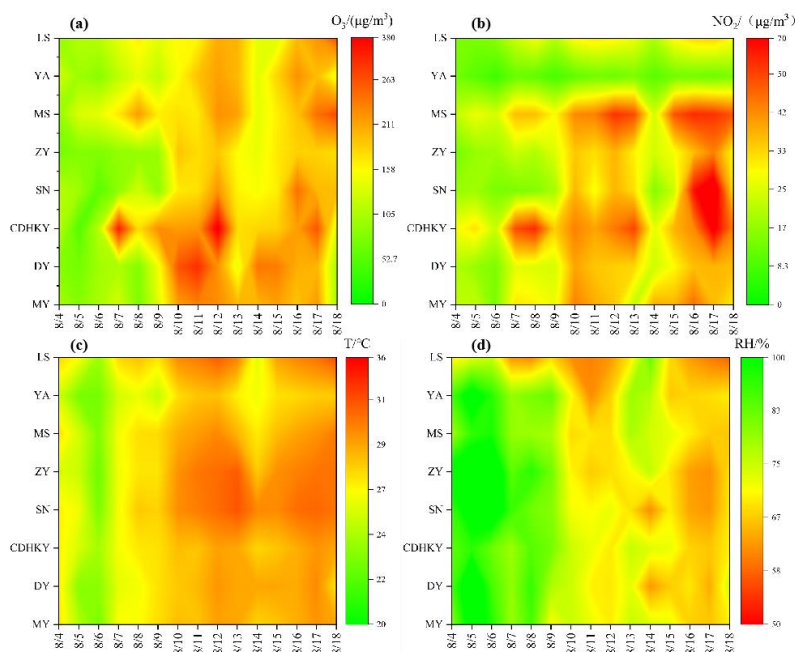
374

375 **Figure 2.** Overview of air quality at each site during the observation period. The gray shaded parts



376

respectively represent the three heavy ozone pollution episodes (EP1,EP2,EP3).



377

378 **Figure 3.** Temporal and spatial variations of (a) ozone concentration, (b) NO₂ concentration, (c)
379 temperature and (d) humidity in the CPOA during the observation period.

380 **3.2 Comparative characterization of carbonyl compounds**

381 **3.2.1 Ambient levels**

382 During the observation period, we utilized 2,4-dinitrophenylhydrazine (DNPH)
383 cartridge and high-performance liquid chromatography (HPLC) analysis technique to
384 quantify 15 carbonyl compounds. The concentrations and relative proportions of these
385 compounds are summarized in Table 1. The average concentration of the 15 carbonyl
386 species in the CPOA was 17.35 ± 5.31 ppb. Overall, areas with elevated concentrations
387 of carbonyl compounds were primarily concentrated in and around Chengdu in both
388 northern and southern directions. MY site, located to the north of Chengdu, exhibited
389 the highest concentration of carbonyl compounds (35.18 ± 13.37 ppb), while YA site,
390 situated southwest of Chengdu, showed the lowest concentration (10.70 ± 4.16 ppb).

391



392 **Table 1.** Daily mean mixing ratio of carbonyl compounds at each site in the CPUA during the
 393 observation period (ppbv)

Carbonyls	MY	DY	CDHKY	XJ	SN	ZY	MS	YA	LS
formaldehyde	12.82±6.52	6.06±2.82	10.09±4.21	8.87±4.39	6.98±3.56	5.84±2.69	8.47±4.15	6.36±2.40	6.55±3.35
acetaldehyde	16.65±7.38	1.54±0.77	3.65±2.15	2.33±1.07	2.62±1.74	1.40±0.61	3.24±1.60	0.88±0.68	1.63±1.32
acetone	4.36±1.70	2.80±1.19	4.51±2.25	3.70±1.21	3.14±1.70	3.23±1.73	2.15±1.14	2.18±1.08	2.91±1.63
propionaldehyde	0.41±0.22	0.24±0.14	0.39±0.27	0.39±0.17	0.34±0.22	0.28±0.14	0.41±0.18	0.20±0.15	0.31±0.16
crotonaldehyde	0.20±0.21	0.10±0.11	0.23±0.34	0.05±0.07	0.23±0.08	0.19±0.27	0.15±0.21	0.36±0.24	0.12±0.24
butyraldehyde	0.22±0.48	0.22±0.28	0.40±0.57	0.94±1.67	0.26±0.18	0.06±0.18	0.44±0.46	0.25±0.16	0.02±0.06
benzaldehyde	0.00±0.04	0.02±0.06	0.04±0.11	0.21±0.20	0.08±0.10	0.00±0.01	0.00±0.01	0.00±0.00	0.01±0.04
isovaleraldehyde	0.01±0.14	0.03±0.09	0.08±0.14	0.08±0.13	0.05±0.10	0.01±0.05	0.68±0.42	0.04±0.07	0.06±0.12
valeraldehyde	0.00±0.00	0.25±0.09	0.30±0.59	0.63±0.36	0.85±0.65	0.00±0.00	0.00±0.00	0.00±0.02	0.77±0.47
o-Tolualdehyde	0.46±0.52	0.36±0.29	0.45±0.19	0.00±0.00	0.00±0.00	0.23±0.17	0.43±0.33	0.18±0.22	0.16±0.17
m-Tolualdehyde	0.00±0.02	0.04±0.10	0.04±0.09	0.17±0.17	0.30±0.13	0.00±0.03	0.00±0.02	0.00±0.02	0.01±0.05
p-Tolualdehyde	0.00±0.00	0.01±0.05	0.01±0.04	0.00±0.00	0.00±0.00	0.00±0.00	0.01±0.04	0.00±0.02	0.00±0.02
hexaldehyde	0.00±0.01	0.34±0.25	0.41±0.69	0.57±0.47	0.95±0.65	0.02±0.18	0.78±0.58	0.00±0.01	0.10±0.32
2,5-dimethylbenzaldehyde	0.01±0.03	0.00±0.01	0.00±0.01	0.05±0.12	0.00±0.00	0.00±0.01	0.01±0.02	0.00±0.01	0.00±0.01
MACR	0.03±0.20	0.14±0.17	0.26±0.34	1.05±1.10	0.26±0.21	0.19±0.16	0.42±0.36	0.24±0.22	0.81±0.88
Sum	35.18±13.37	12.16±4.84	20.84±8.85	19.04±8.1	16.05±7.73	11.47±4.89	17.19±7.61	10.70±4.16	13.46±6.12

394

395



396

397 Fig.S1 illustrates the relationship between ozone concentration and carbonyl
398 compounds concentration at each site during the observation period. It is evident that
399 the spatial distribution of carbonyl compound concentrations is similar to that of ozone
400 concentration. Regions with severe ozone pollution tend to exhibit higher
401 concentrations of carbonyl compounds. The variation in carbonyl compound
402 concentrations is primarily attributed to anthropogenic emissions and prevailing
403 summer wind directions in the CUPA. Chengdu is the most economically developed
404 city in the CUPA, with notably higher GDP and industrial production values than other
405 regions. Chengdu's major industries include coal-fired power plants, chemical plants,
406 metallurgy and building materials plants, and high concentrations of carbonyls were
407 observed in here. The unique basin climate of the CUPA, characterized by intense
408 sunlight and stable atmospheric conditions, facilitates the accumulation of pollutants.
409 Large amount of industrial emissions and strong photochemical reaction contributes to
410 ozone pollution. Additionally, during the summer, prevailing northerly winds in the
411 CUPA facilitate the downwind transport of pollutants from upwind sources, leading to
412 regional pollution. It is noteworthy that the concentration of carbonyl compounds at the
413 MY site significantly exceeds that at the CDHKY site. MY, with its industrial roots,
414 consistently maintains its position as the second-highest GDP contributor in Sichuan
415 Province. The electronics information industry stands as Mianyang's primary economic
416 driver, constituting approximately half of the city's total output value. Studies
417 investigating the volatile organic compound (VOC) source profile in Chengdu(Zhou et
418 al., 2021) reveal that ethanol and carbonyls predominantly characterize electronics
419 manufacturing emissions.

420 3.2.2 Compositional characteristics

421 According to the composition characteristics of 15 carbonyl compounds in the
422 ambient air of each city during the observation period (Table S4) . Formaldehyde was



423 the most abundant specie found in these sites followed by acetone and acetaldehyde,
424 which is widely observed in previous studies. The concentration ratios of formaldehyde,
425 acetone, and acetaldehyde across different sites ranged from 36.4% to 59.4% (average
426 48.1%), 12.4% to 28.1% (average 19.9%), and 8.2% to 47.3% (average 17.5%),
427 respectively. In this study, the total concentrations of formaldehyde, acetaldehyde, and
428 acetone (FAT) account for over 78% of the total carbonyls concentrations. At the MY
429 and ZY sites, this proportion even exceeded 90%. It is noteworthy that isobutyraldehyde
430 (MACR) ranks fourth in the volume concentration of 15 carbonyls in the ambient air
431 surrounding XJ, accounting for 5.3%. MACR, a characteristic product of isoprene
432 photooxidation from biogenic sources, possibly originates from the abundant
433 vegetation surrounding XJ. It reflects the period's relatively active photochemical
434 reactions, with substantial contributions from secondary formation to the carbonyls
435 composition.

436 The observed levels of FAT in different areas were influenced by various factors
437 including sampling period, geographic location, meteorological conditions, chemical
438 removal, and source emissions(Z. Zhang et al., 2016). Despite these influences,
439 comparisons remain valuable in providing an overview of ambient carbonyl levels in
440 the CPUA. During the summer of 2010, a national wide survey of ambient
441 monocarbonyl compounds were conducted simultaneously in nine sites (Ho et al.,
442 2015)found that the total FAT concentration was highest in Chengdu (14.96 ppb),
443 followed by Beijing (11.83 ppb), and Wuhan (11.70 ppb). Beijing, as the capital of
444 China, and Wuhan, being one of the top ten most populous cities in China, played
445 significant roles in this comparison. In our study, the CDHKY site within CPUA
446 exhibited the highest FAT concentration, with values of 18.25 ppb, surpassing those
447 recorded in 2010. Furthermore, the total FAT concentrations observed at the CPUA and
448 XJ sites, with values of 14.99 ppb and 14.90 ppb respectively in our study, closely
449 resemble those reported in August 2010 in Chengdu. This suggests that elevated
450 concentrations of carbonyl compounds in Chengdu have been a longstanding issue on



451 a national scale. Comparing our findings to international studies, the FAT
452 concentrations at the CDHKY site were lower than those reported in Rio De Janeiro,
453 Brazil(da Silva et al., 2016), during July to October 2013 (35.43 ppb), but higher than
454 those in Bangkok, Thailand(Kanjanasiranont et al., 2016b), Orleans, France(Jiang et al.,
455 2016), and the United States(Murillo et al., 2012), with values of 9.05 ppb, 6.12 ppb,
456 and 5.76 ppb, respectively.

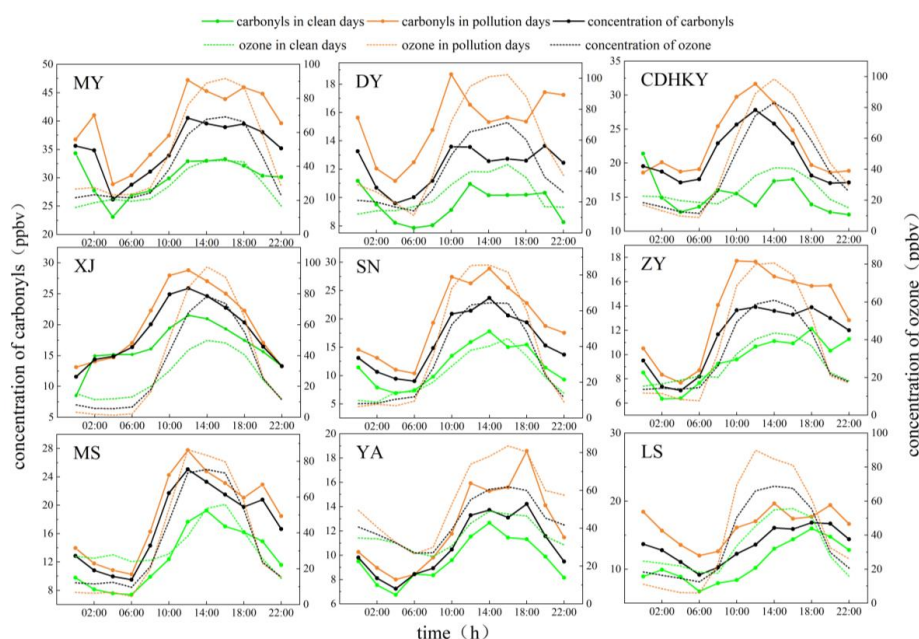
457 3.3 Temporal variations of carbonyl compounds

458 The diurnal variation of the total mixing ratio of ambient carbonyl compounds and
459 ozone concentration around each site in the CPUA during the observation period is
460 shown in Fig. 4. According to the observation results, the diurnal trend of ozone
461 concentration at each site showed a "unimodal" variation characteristic, that was, it
462 gradually increased from the morning to the peak of one day at noon, and then decreased.
463 The diurnal variation of the total mixing ratio of carbonyl compounds at each site
464 generally showed a characteristic of high during the daytime and low at night. The
465 concentration of carbonyl compounds during the day (6:00-16:00) was 48.8% higher
466 than that at night (18:00-4:00) at the XJ site. This indicated that the concentration of
467 carbonyl compounds increased by photochemical production during the daytime. The
468 diurnal variation characteristics of each site were different. For example, the diurnal
469 variation characteristics of carbonyl compounds concentration at CDHKY, XJ and SN
470 sites were consistent with those of ozone. The diurnal variation of carbonyl compounds
471 concentrations at other sites showed "double peaks", peaking at 10:00-12:00 and 18:00-
472 20:00, respectively. The concentrations of carbonyl compounds at night were also
473 higher at MY, DY and LS sites. The diurnal minimum values of the total concentration
474 of carbonyl compounds and ozone concentration appeared at similar time, usually at
475 4:00 a.m. or 6:00 a.m. The first peak of the total mixing ratio of carbonyl compounds
476 occurred earlier than the maximum ozone concentration of the day. The first peak of
477 the total mixing ratio of carbonyl compounds mostly occurred between 10:00 and 12:00.
478 And the maximum ozone concentration mostly occurs between 14:00 and 16:00. This



479 was related to the fact that carbonyl compounds were important precursors of ozone.

480 In general, the diurnal variation of the total concentration of carbonyl
 481 compounds on pollution days and clean days was high during the daytime and low at
 482 night. The total mixing ratio of carbonyl compounds on pollution days was 22.8%-
 483 66.2% higher than that on clean days. At the same time, the increase of concentration
 484 of carbonyl compounds during the daytime on pollution days was higher than that on
 485 clean days. This suggested that the increase in the concentration of carbonyl
 486 compounds during the daytime contributed to ozone pollution.



487
 488 **Figure 4.** Diurnal variations of carbonyl compounds and ozone concentrations at each site in the
 489 CPUA during the observation period

490 The diurnal variation of the mixing ratio of ambient carbonyl compounds on
 491 weekdays and weekends in the eight cities of the CPUA is shown in Fig. S2. The total
 492 concentration of carbonyl compounds at each site on weekends was higher than that on
 493 weekdays, and the increase in carbonyl compounds at 0:00 (36.3%), 10:00 (16.3%) and
 494 18:00-22:00 (17.6%) on weekends was higher than that on weekdays. Except for the
 495 XJ site, the increase in the concentration of carbonyl compounds at 0:00 on weekends



496 was significantly higher than that on weekdays, which was mainly related to the
497 increase of acetaldehyde, propionaldehyde and acetone on weekends. At 10:00, the
498 higher increase at DY, CDHKY and SN sites was mainly related to the increase of
499 propionaldehyde, acetaldehyde and formaldehyde concentrations. From 18:00 to 22:00,
500 the higher increase at DY and YA sites was mainly related to the increase in the
501 concentrations of propionaldehyde, acetone and acetaldehyde. Acetaldehyde, acetone
502 and propionaldehyde were mainly from vehicle exhaust. In particular, when ethanol
503 gasoline and biodiesel were used as alternative fuels, the content of acetaldehyde and
504 acetone in the exhaust gas would be significantly increased. Therefore, the increase in
505 the concentration of carbonyl compounds on weekends might be related to the increase
506 in traffic at 10:00 and at night. In addition, the peak concentration of carbonyl
507 compounds on weekends (10:00) was earlier than that on weekdays (12:00-14:00) at
508 CDHKY, XJ and SN sites, and the diurnal trend of carbonyl compounds concentrations
509 on weekdays and weekends had little difference at other sites.

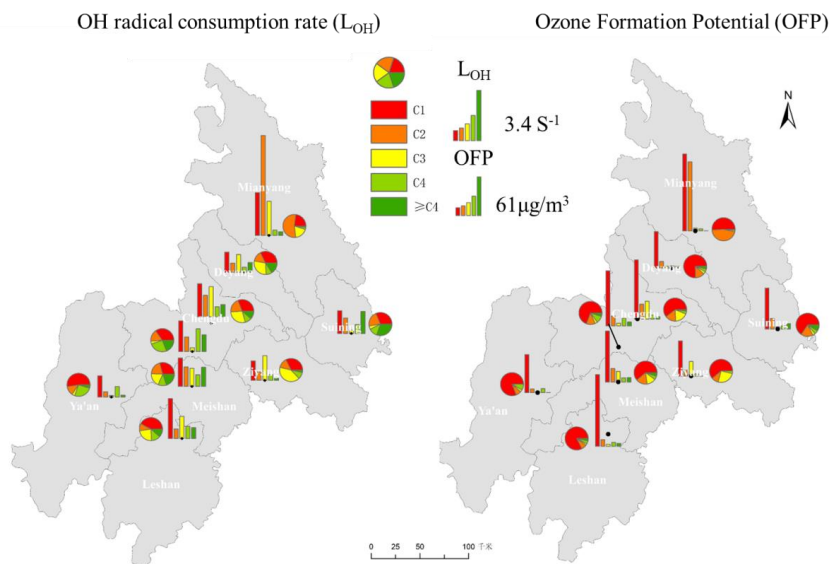
510 3.4 Atmospheric photochemical reactivity of carbonyl compounds

511 During the observation period, the total OH radical consumption rate (L_{OH}) and
512 total ozone formation potential (OFP) of the 15 carbonyl compounds at each site are
513 depicted in Fig.5. The ranking of total L_{OH} and total OFP at each site is consistent,
514 except for the YA and ZY sites with lower concentrations of carbonyl compounds,
515 where the atmospheric photochemical reactivity ranking also aligns with the
516 concentration. Among all sites, the MY and CD sites display the highest reactivity,
517 while the YA and ZY sites exhibit the lowest reactivity. Contrasting the L_{OH} and OFP
518 during clean and polluted periods reveals higher values during ozone pollution periods
519 than clean days. L_{OH} and OFP during different pollution periods show a strong positive
520 correlation with the severity of ozone pollution; the heavier the ozone pollution, the
521 higher the L_{OH} and OFP at the sites. Regardless of clean or polluted periods, the L_{OH}
522 and OFP at the MY site are higher than other sites. However, despite this, the average
523 ozone concentration at the MY site ranks lower among the nine sites observed. This



524 might be associated with higher concentrations of aldehyde compounds at the MY site.

525 During the observation period, carbonyl compounds significantly contributed to
 526 ozone formation. The contributions to total VOCs (alkanes, alkenes, alkynes, aromatics,
 527 and carbonyl compounds) OFP at the MY, SN, ZY, YA, and LS sites ranged from 19.5%
 528 to 48.6%. Formaldehyde and acetaldehyde were identified as the most reactive species
 529 in the atmosphere, surpassing other carbonyl compounds in reactivity due to their
 530 higher concentrations and inherent reactivity, especially formaldehyde. However,
 531 acetone exhibited high inertness and a prolonged atmospheric lifetime, leading to its
 532 accumulation in ambient air with concentrations higher than other carbonyl compounds
 533 except for formaldehyde and acetaldehyde. Thus, despite its elevated concentration,
 534 acetone's reactivity remained relatively low.



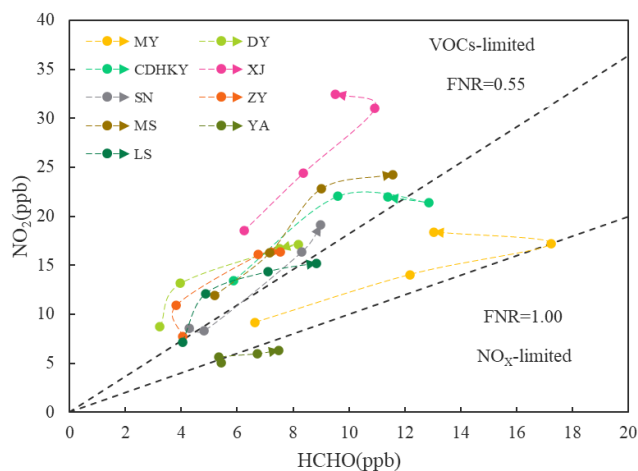
535
 536 **Figure 5.** L_{OH} and OFP of carbonyl compounds at each site in the CUPA during the observation
 537 period

538 3.5 Sensitivity analysis of ozone formation based on formaldehyde to NO_2 ratio (FNR)

539 The change of O_3 formation sensitivity of each site in the CUPA during the
 540 observation period is shown in Fig.3.9. As can be seen from the Fig. 6, most sites remain



541 in the VOCs-limited regime during the cleaning period and EP1 to EP3. Economically
 542 developed city such as Chengdu, Meishan, with high levels of formaldehyde and NO₂,
 543 remain in the VOCs-limited regime. Ya'an as a city with the lowest GDP ranking in the
 544 CPUA, with low levels of formaldehyde and NO₂, remain in the transitional regime.



545

546 **Figure 6.** The change of O₃ formation sensitivity of each site in the CPUA during the observation
 547 period. The arrows represent time step from clean period to EP1 to EP2 to EP3.

548 The daily variation of O₃ formation sensitivity and ozone concentration at each
 549 site in the CPUA during the observation period is shown in Fig. S5. The mean FNR of
 550 each site ranged from 0.48 to 1.29 during the observation period. The FNRs were lower
 551 than 0.55±0.16 at XJ, DY, ZY, CDHKY, and MS, and higher than 1.0 at LS, SN, YA and
 552 MY. At the same time, the mean ozone concentration at each site was between 138 and
 553 192 µg/m³. The mean ozone concentration in XJ, DY, CDHKY and MS was 166-192
 554 µg/m³, it was 150-164 µg/m³ in LS, SN, YA and MY. Therefore, it could be seen that
 555 most of the sites with high mean ozone concentrations during the observation period,
 556 like CDHKY, XJ, MS and Deyan sites, were in the VOCs-limited regime, and most of
 557 the stations with low mean ozone concentrations during the observation period such as
 558 YA, SN, MY and LS were in the transitional regime. It was worth noting that the mean
 559 ozone concentration at ZY site (only 138 µg/m³) during the observation period was
 560 much lower than that of other sites, but most of the ZY site was in VOCs-limited regime,



561 which was mainly related to the low concentration of formaldehyde. In addition, the
562 FNR value of the MY site was also relatively high, which was mainly caused by the
563 high concentration of formaldehyde.

564 Based on the ratio of formaldehyde to NO₂ mixing ratio, most sites remain in the
565 VOCs-limited regime during the observation period. And the sites with heavy ozone
566 pollution were in the VOCs-limited regime, and the sites with light ozone pollution
567 were in the transitional regime. Photochemical reactivity (L_{OH} and OFP) analysis
568 showed that formaldehyde and acetaldehyde contributed significantly to the
569 enhancement of atmospheric oxidation and ozone formation potential. Therefore, when
570 heavy ozone pollution occurs in the CPUA, special attention should be paid to the
571 control of VOCs, especially formaldehyde and acetaldehyde in carbonyl compounds,
572 under the coordinated control of NO_x and VOCs. Overall, this study reveals the
573 important contribution of carbonyl compounds to ozone pollution in the CPUA, and
574 provides scientific support for the establishment of ozone pollution prevention and
575 control measures.

576 3.6 Source Analysis of carbonyl compounds

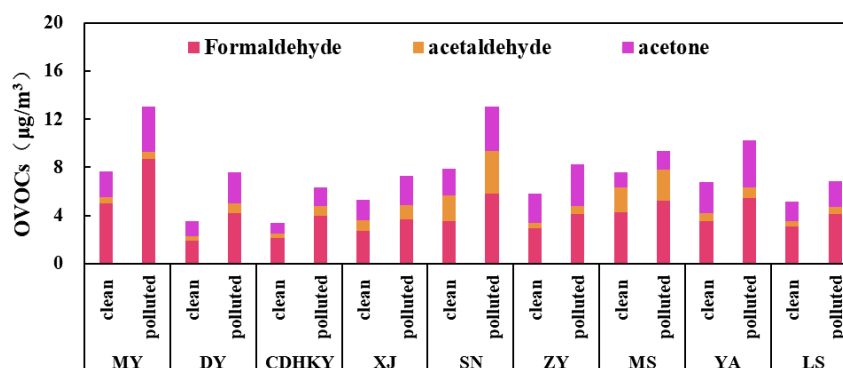
577 3.6.1 Quantitative source analysis of key carbonyl compounds

578 The table S7 provides a summary of the background and primary emissions
579 concentrations of formaldehyde, acetaldehyde, and acetone at nine sites across the eight
580 cities of the CPUA, along with the proportion of secondary formation contributing to
581 their concentrations. Background concentrations and primary emissions of
582 formaldehyde, acetaldehyde, and acetone ranged from 50% to 80%, 46% to 83%, and
583 45% to 78%, respectively. Secondary formation accounted for 20% to 50%, 17% to
584 54%, and 22% to 55% of their concentrations, respectively. Notably, in SN and YA, the
585 secondary formation of formaldehyde contributed half of the observed concentration,
586 indicating it as the predominant source, while acetaldehyde's secondary formation also
587 prevailed in these sites. Conversely, acetone, with lower reactivity, primarily originated



588 from background concentrations and primary emissions at other sites except YA.
 589 Moreover, background concentrations and primary emissions were identified as the
 590 main contributors to carbonyl compounds in XJ and LS.

591 Fig.7 illustrates the secondary formation concentrations of formaldehyde,
 592 acetaldehyde, and acetone at each site in the CPUA under both clean and polluted
 593 conditions. Under polluted conditions, the secondary concentrations of formaldehyde,
 594 acetaldehyde, and acetone exceeded those in clean conditions by 52.4%, 80.3%, and
 595 58.5%, respectively. The most significant increases in secondary concentrations were
 596 observed at the SN site, while relatively smaller increases were observed at LS and XJ.



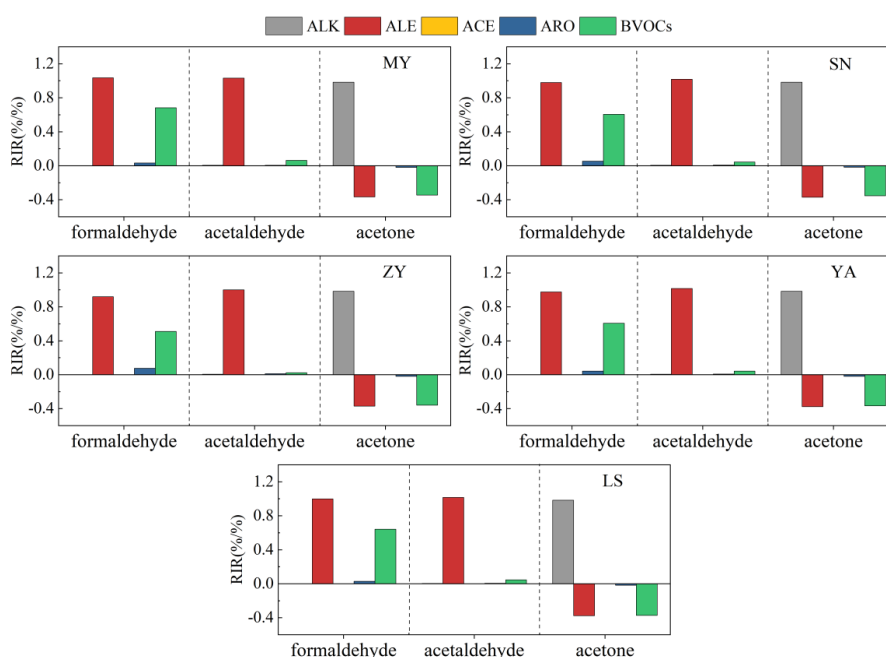
597
 598 **Figure 7.** Concentrations of formaldehyde, acetaldehyde and acetone in secondary formation
 599 under different pollution conditions at each site in the CPUA during the observation period

600 3.6.2 Investigation of secondary formation mechanism of key carbonyl compounds

601 The effects of anthropogenic source VOCs and plant source VOCs on the
 602 formation of formaldehyde, acetaldehyde and acetone at MY, SN, ZY, YA and LS sites
 603 were researched during a regional ozone pollution period when all 8 cities of the CPUA
 604 had mild or above ozone pollution (August 11th, 12th and 16th) (Fig.8). Overall, the
 605 sensitivities of different anthropogenic source and plant source VOCs to formaldehyde,
 606 acetaldehyde and acetone was consistent among sites. For formaldehyde, reducing
 607 alkenes in anthropogenic source VOCs and plant VOCs was the most effective way to
 608 control formaldehyde concentration, while reducing alkenes in anthropogenic source



609 VOCs was also beneficial to reduce the formation of acetaldehyde. For acetone with
 610 low reactivity, the alkanes in anthropogenic source VOCs were the most sensitive to
 611 the formation of acetone, followed by alkenes and BVOCs. Only the RIR value of
 612 alkanes were greater than zero, and the RIR values of both alkenes and BVOCs were
 613 less than zero, indicating that reducing alkanes could reduce the formation of acetone,
 614 while reducing alkenes and BVOCs was not conducive to acetone concentration control.



615
 616 **Figure 8.** Mean RIRs of formaldehyde, acetaldehyde and acetone to different anthropogenic
 617 source VOCs and biogenic source VOCs at MY, SN, ZY, YA and LS sites on August 11th, 12th and
 618 16th

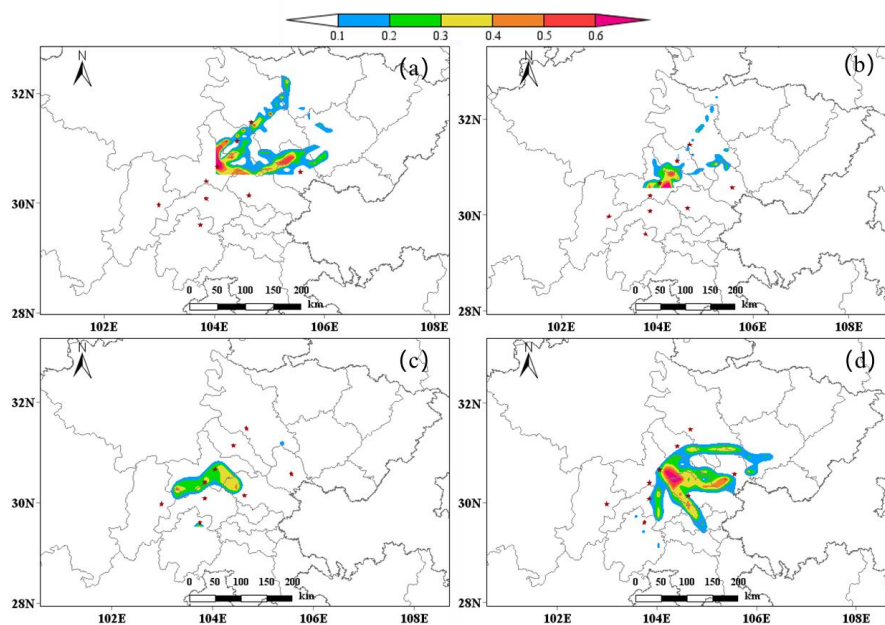
619 3.6.3 Influence of regional transportation contribution

620 The TrajStat trajectory model was used to calculate and cluster the 24-hour
 621 backward trajectories of air quality at the sampling sites. The backward trajectory
 622 during sampling is shown in Fig.S6. During the observation period, the pollution of
 623 carbonyl compounds in the cities of the CPUA was affected by the mutual transport
 624 among cities in Sichuan Province, especially along the MY-DY-CDHKY route. In



625 addition, the surrounding provinces and cities of Sichuan Province (Gansu and
626 Chongqing) also contributed to the carbonyl compounds of the CPUA.

627 The potential sources of carbonyl compounds at different pollution stages at the
628 Chengdu Institute of Environmental Sciences site during the observation period are
629 shown in Fig. 9. It can be seen from the figure that there are differences in the potential
630 sources of carbonyl compounds among different pollution stages at the CDHKY site.
631 The concentration of local carbonyl compounds in CDHKY was high during the early
632 observation period and EP1, which existed local sources, and was also affected by the
633 northern airflow, and carbonyl compounds was also affected by the transport from MY,
634 DY and other northern regions. Under the effect of the continuous northern airflow, the
635 local source emissions decreased during EP1, and the potential source of carbonyl
636 compounds changed to from the junction between CDHKY and ZY. During EP3, under
637 the combined influence of the western airflow, the contribution of transport from SN
638 and ZY to carbonyl compounds increased, while emissions from local sources also
639 increased.



640
641 **Figure 9.** Analysis of potential sources of carbonyl compounds at different periods at the CDHKY



642 site during the observation period (a) August 4th-6th (b) August 7th-9th (c) August 10th-13th (d)
643 August 15th-18th

644 4. Conclusions

645 During a concurrent atmospheric observation campaign conducted at nine sites in
646 the CPOA from August 4th to 18th, 2019, three regional heavy ozone pollution episodes,
647 labeled EP1 to EP3, were observed. This study extensively examines the concentration
648 variations, atmospheric chemical reactivity, and sources of carbonyls during this period.
649 The average total concentrations of 15 carbonyl compounds across the nine sites within
650 eight cities of the CPOA were measured at 17.35 ± 5.31 ppb. Spatial analysis revealed
651 a positive correlation between carbonyl levels and ozone concentrations, particularly
652 concentrated around Chengdu in both northern and southern directions. Formaldehyde
653 (36.4%-64.3%), acetone (12.4%-28.1%), and acetaldehyde (8.2%-47.3%) constituted
654 the predominant species by volume concentration. Intriguingly, Chengdu exhibited FAT
655 concentrations surpassing national and international levels, indicating heightened levels
656 compared to other regions. Diurnal variations showed peaks during the day and lows at
657 night, with notable spikes on ozone pollution days. A distinctive "weekend effect" was
658 observed, particularly evident in carbonyl compounds associated with motor vehicle
659 emissions, such as acetaldehyde and acetone, peaking during morning rush hours and
660 nighttime on weekends. This suggests significant contributions from both daytime
661 photochemical processes and nighttime vehicular emissions to carbonyl compounds. At
662 the MY site, 48.6% of the total volatile organic compounds (VOCs) ozone formation
663 potential (OFP) was attributed to the 15 carbonyl compounds, emphasizing their
664 substantial impact on ozone formation, especially formaldehyde and acetaldehyde.

665 Ground-level observations of FNR were utilized to assess the sensitivity of
666 ground-level ozone formation. FNR from ground-level observations were used to
667 determine the sensitivity of ground-level ozone formation. Analysis of FNR revealed
668 that sites experiencing heavy ozone pollution exhibited lower FNRs, indicating a



669 VOCs-limited regime, while sites with lighter ozone pollution were categorized into a
670 transitional regime. Carbonyl compound sources include primary emissions and
671 secondary formation processes. Multivariate linear regression quantitatively analyzed
672 formaldehyde, acetaldehyde, and acetone sources. Secondary formation contributed
673 over 30% on average to formaldehyde, acetaldehyde, and acetone, despite primary
674 emissions being primary sources. OBM modeling revealed that formaldehyde and
675 acetaldehyde primarily originated from the secondary formation of alkenes and BVOCs,
676 while acetone mainly stemmed from the secondary formation of alkanes. Furthermore,
677 it is recommended to establish a scientific control mechanism for both NO_x and VOCs,
678 with special attention to formaldehyde, acetaldehyde, and acetone, and their alkenes
679 precursors. Additionally, considering the regional nature of pollution, this study
680 suggests that carbonyl compound pollution is influenced by mutual transport among
681 cities within the CPUA, notably along the MY-DY-CDHKY route. Establishing a
682 collaborative prevention and control mechanism among cities within the CPUA and
683 neighboring provinces and cities is crucial to effectively address carbonyl compounds
684 and ozone pollution in the region in the future.

685

686 **Data availability.** Observational data including meteorological parameters and air
687 pollutants used in this study are available from the corresponding authors upon request
688 (lihong@craes.org.cn).

689

690 **Author contributions.** Hong Li and Jiemeng Bao designed this study. Xin Zhang,
691 Zhenhai Wu, Jiemeng Bao, Li Zhou, Qinwen Tan, and Fumo Yang coordinated the
692 selection of field observation sites, including locations for both VOCs and carbonyls
693 grid sampling. Qinwen Tan and Hefan Liu supported the collection of carbonyls at one
694 site. Zhenhai Wu and Xin Zhang assisted in carbonyls sampling; Xin Zhang and
695 Yunfeng Li assisted in carbonyls sample analysis and data collection. Li Zhou and
696 Hefan Liu organized the analysis of VOCs measurements. Jun Qian, Junhui Chen, and



697 Liqun Deng provided support in project funding application. Jiemeng Bao performed
698 the data analysis and wrote the paper with contributions from all co-authors; Hong Li
699 reviewed the paper, provided comments and finalized it.

700

701 **Competing interests.** The contact author has declared that none of the authors has any
702 competing interests.

703

704 **Acknowledgments.** The authors would like to express their sincere appreciation to
705 Keding Lu and Xin Li of Peking University for their organization of the intensive field
706 observation experiment on the formation mechanisms of photochemical pollution in
707 summer in the CPUA of China. They also want to show their deep gratitude to Yulei
708 Ma, Tianli Song, Xiaodong Wu, Ning Wang, and He Zijun Liu of Sichuan University,
709 as well as Xin Zhang (female) and Hefan Liu of Chengdu Academy of Environmental
710 Protection Sciences for their help in sampling. They are also grateful to Liping Liu of
711 Sichuan Agricultural University in Ya'an City, Kaiyao Lv of Mianyang High-tech Zone
712 Management Committee, Yong Xiao of Deyang Municipal Education Bureau, Ying Ni
713 of Meishan Ecological Environment Bureau, Aihua Zou of Leshan Ecological
714 Environment Bureau, and Chuhan Wang of the Chinese Academy of Environmental
715 Sciences for their substantial support during field observations. Special thanks to Zhen
716 He and Manfei Yin of the Chinese Academy of Environmental Sciences for their
717 assistance in analyzing samples from the XJ site.

718

719 **Financial support.** This research has been supported by the Research Project on
720 Analysis of Multiple Causes of Atmospheric Ozone Pollution in Urban Agglomerations
721 of Chengdu Plain and Development of Management, Prevention, and Control System
722 of Sichuan Academy of Environmental Sciences (No. 510201201905430).

723

724 **References**



- 725 Atkinson, R., Arey, J., 2003. Atmospheric Degradation of Volatile Organic Compounds.
726 Chem. Rev. 103, 4605–4638. <https://doi.org/10.1021/cr0206420>
- 727 Bao, J., Li, H., Wu, Z., Zhang, X., Zhang, H., Li, Y., Qian, J., Chen, J., Deng, L., 2022.
728 Atmospheric carbonyls in a heavy ozone pollution episode at a metropolis in
729 Southwest China: Characteristics, health risk assessment, sources analysis.
730 Journal of Environmental Sciences 113, 40–54.
731 <https://doi.org/10.1016/j.jes.2021.05.029>
- 732 da Silva, D.B.N., Martins, E.M., Corrêa, S.M., 2016. Role of carbonyls and aromatics
733 in the formation of tropospheric ozone in Rio de Janeiro, Brazil. Environ Monit
734 Assess 188, 289. <https://doi.org/10.1007/s10661-016-5278-3>
- 735 Duan, J., Guo, S., Tan, J., Wang, S., Chai, F., 2012. Characteristics of atmospheric
736 carbonyls during haze days in Beijing, China. Atmospheric Research 114–115,
737 17–27. <https://doi.org/10.1016/j.atmosres.2012.05.010>
- 738 Duan, J., Tan, J., Yang, L., Wu, S., Hao, J., 2008. Concentration, sources and ozone
739 formation potential of volatile organic compounds (VOCs) during ozone
740 episode in Beijing. Atmospheric Research 88, 25–35.
741 <https://doi.org/10.1016/j.atmosres.2007.09.004>
- 742 Fu, T.-M., Jacob, D.J., Wittrock, F., Burrows, J.P., Vrekoussis, M., Henze, D.K., 2008.
743 Global budgets of atmospheric glyoxal and methylglyoxal, and implications for
744 formation of secondary organic aerosols. Journal of Geophysical Research:
745 Atmospheres 113. <https://doi.org/10.1029/2007JD009505>
- 746 Fuchs, H., Tan, Z., Lu, K., Bohn, B., Broch, S., Brown, S.S., Dong, H., Gomm, S.,
747 Häsel, R., He, L., Hofzumahaus, A., Holland, F., Li, X., Liu, Y., Lu, S., Min,
748 K.-E., Rohrer, F., Shao, M., Wang, B., Wang, M., Wu, Y., Zeng, L., Zhang,
749 Yinson, Wahner, A., Zhang, Yuanhang, 2017. OH reactivity at a rural site
750 (Wangdu) in the North China Plain: contributions from OH reactants and
751 experimental OH budget. Atmospheric Chemistry and Physics 17, 645–661.
752 <https://doi.org/10.5194/acp-17-645-2017>
- 753 Guenther, A.B., Jiang, X., Heald, C.L., Sakulyanontvittaya, T., Duhl, T., Emmons, L.K.,
754 Wang, X., 2012. The Model of Emissions of Gases and Aerosols from Nature
755 version 2.1 (MEGAN2.1): an extended and updated framework for modeling
756 biogenic emissions. Geoscientific Model Development 5, 1471–1492.
757 <https://doi.org/10.5194/gmd-5-1471-2012>
- 758 Guo, H., Wang, T., Simpson, I.J., Blake, D.R., Yu, X.M., Kwok, Y.H., Li, Y.S., 2004.
759 Source contributions to ambient VOCs and CO at a rural site in eastern China.
760 Atmospheric Environment 38, 4551–4560.
761 <https://doi.org/10.1016/j.atmosenv.2004.05.004>
- 762 Ho, K.F., Ho, S.S.H., Huang, R.-J., Dai, W.T., Cao, J.J., Tian, L., Deng, W.J., 2015.
763 Spatiotemporal distribution of carbonyl compounds in China. Environmental
764 Pollution 197, 316–324. <https://doi.org/10.1016/j.envpol.2014.11.014>
- 765 Hong, Q., Zhu, L., Xing, C., Hu, Q., Lin, H., Zhang, C., Zhao, C., Liu, T., Su, W., Liu,
766 C., 2022. Inferring vertical variability and diurnal evolution of O₃ formation
767 sensitivity based on the vertical distribution of summertime HCHO and NO₂ in
768 Guangzhou, China. Science of The Total Environment 827, 154045.



- 769 <https://doi.org/10.1016/j.scitotenv.2022.154045>
- 770 Hu, J., Wang, P., Ying, Q., Zhang, H., Chen, J., Ge, X., Li, X., Jiang, J., Wang, S., Zhang,
771 J., Zhao, Y., Zhang, Y., 2017. Modeling biogenic and anthropogenic secondary
772 organic aerosol in China. *Atmospheric Chemistry and Physics* 17, 77–92.
773 <https://doi.org/10.5194/acp-17-77-2017>
- 774 Jiang, Z., Grosselin, B., Daële, V., Mellouki, A., Mu, Y., 2016. Seasonal, diurnal and
775 nocturnal variations of carbonyl compounds in the semi-urban environment of
776 Orléans, France. *Journal of Environmental Sciences, Changing Complexity of*
777 *Air Pollution* 40, 84–91. <https://doi.org/10.1016/j.jes.2015.11.016>
- 778 Kanjanasiranont, N., Prueksasit, T., Morknoy, D., Tunsaringkarn, T., Sematong, S.,
779 Siritwong, W., Zapaung, K., Rungsiyothin, A., 2016a. Determination of ambient
780 air concentrations and personal exposure risk levels of outdoor workers to
781 carbonyl compounds and BTEX in the inner city of Bangkok, Thailand.
782 *Atmospheric Pollution Research* 7, 268–277.
783 <https://doi.org/10.1016/j.apr.2015.10.008>
- 784 Kanjanasiranont, N., Prueksasit, T., Morknoy, D., Tunsaringkarn, T., Sematong, S.,
785 Siritwong, W., Zapaung, K., Rungsiyothin, A., 2016b. Determination of ambient
786 air concentrations and personal exposure risk levels of outdoor workers to
787 carbonyl compounds and BTEX in the inner city of Bangkok, Thailand.
788 *Atmospheric Pollution Research* 7, 268–277.
789 <https://doi.org/10.1016/j.apr.2015.10.008>
- 790 Li, N., Fu, T.-M., Cao, J., Lee, S., Huang, X.-F., He, L.-Y., Ho, K.-F., Fu, J.S., Lam, Y.-
791 F., 2013. Sources of secondary organic aerosols in the Pearl River Delta region
792 in fall: Contributions from the aqueous reactive uptake of dicarbonyls.
793 *Atmospheric Environment, Improving Regional Air Quality over the Pearl*
794 *River Delta and Hong Kong: from Science to Policy* 76, 200–207.
795 <https://doi.org/10.1016/j.atmosenv.2012.12.005>
- 796 Li, Y., Shao, M., Lu, S., Chang, C.-C., Dasgupta, P.K., 2010. Variations and sources of
797 ambient formaldehyde for the 2008 Beijing Olympic games. *Atmospheric*
798 *Environment* 44, 2632–2639. <https://doi.org/10.1016/j.atmosenv.2010.03.045>
- 799 Ling, Z.H., Zhao, J., Fan, S.J., Wang, X.M., 2017. Sources of formaldehyde and their
800 contributions to photochemical O₃ formation at an urban site in the Pearl River
801 Delta, southern China. *Chemosphere* 168, 1293–1301.
802 <https://doi.org/10.1016/j.chemosphere.2016.11.140>
- 803 Liu, J., Li, X., Tan, Z., Wang, W., Yang, Y., Zhu, Y., Yang, S., Song, M., Chen, S., Wang,
804 H., Lu, K., Zeng, L., Zhang, Y., 2021. Assessing the Ratios of Formaldehyde
805 and Glyoxal to NO₂ as Indicators of O₃–NO_x–VOC Sensitivity. *Environ. Sci.*
806 *Technol.* 55, 10935–10945. <https://doi.org/10.1021/acs.est.0c07506>
- 807 Lou, S., Holland, F., Rohrer, F., Lu, K., Bohn, B., Brauers, T., Chang, C.C., Fuchs, H.,
808 Häsel, R., Kita, K., Kondo, Y., Li, X., Shao, M., Zeng, L., Wahner, A., Zhang,
809 Y., Wang, W., Hofzumahaus, A., 2010. Atmospheric OH reactivities in the Pearl
810 River Delta – China in summer 2006: measurement and model results.
811 *Atmospheric Chemistry and Physics* 10, 11243–11260.
812 <https://doi.org/10.5194/acp-10-11243-2010>



- 813 Luecken, D.J., Hutzell, W.T., Strum, M.L., Pouliot, G.A., 2012. Regional sources of
814 atmospheric formaldehyde and acetaldehyde, and implications for atmospheric
815 modeling. *Atmospheric Environment* 47, 477–490.
816 <https://doi.org/10.1016/j.atmosenv.2011.10.005>
- 817 Lui, K.H., Ho, S.S.H., Louie, P.K.K., Chan, C.S., Lee, S.C., Hu, D., Chan, P.W., Lee,
818 J.C.W., Ho, K.F., 2017. Seasonal behavior of carbonyls and source
819 characterization of formaldehyde (HCHO) in ambient air. *Atmospheric*
820 *Environment* 152, 51–60. <https://doi.org/10.1016/j.atmosenv.2016.12.004>
- 821 Murillo, J.H., Marín, J.F.R., Román, S.R., 2012. Determination of carbonyls and their
822 sources in three sites of the metropolitan area of Costa Rica, Central America.
823 *Environ Monit Assess* 184, 53–61. <https://doi.org/10.1007/s10661-011-1946-5>
- 824 Pang, X., Mu, Y., 2006. Seasonal and diurnal variations of carbonyl compounds in
825 Beijing ambient air. *Atmospheric Environment* 40, 6313–6320.
826 <https://doi.org/10.1016/j.atmosenv.2006.05.044>
- 827 Rao, Z., Chen, Z., Liang, H., Huang, L., Huang, D., 2016. Carbonyl compounds over
828 urban Beijing: Concentrations on haze and non-haze days and effects on radical
829 chemistry. *Atmospheric Environment, Air Pollution in the Beijing – Tianjin –*
830 *Hebei (BTH) region, China* 124, 207–216.
831 <https://doi.org/10.1016/j.atmosenv.2015.06.050>
- 832 Schroeder, J.R., Crawford, J.H., Fried, A., Walega, J., Weinheimer, A., Wisthaler, A.,
833 Müller, M., Mikoviny, T., Chen, G., Shook, M., Blake, D.R., Tonnesen, G.S.,
834 2017. New insights into the column CH₂O/NO₂ ratio as an indicator of near-
835 surface ozone sensitivity. *Journal of Geophysical Research: Atmospheres* 122,
836 8885–8907. <https://doi.org/10.1002/2017JD026781>
- 837 Shao, M., Lu, S., Liu, Y., Xie, X., Chang, C., Huang, S., Chen, Z., 2009. Volatile organic
838 compounds measured in summer in Beijing and their role in ground-level ozone
839 formation. *Journal of Geophysical Research: Atmospheres* 114.
840 <https://doi.org/10.1029/2008JD010863>
- 841 Shen, X., Zhao, Y., Chen, Z., Huang, D., 2013. Heterogeneous reactions of volatile
842 organic compounds in the atmosphere. *Atmospheric Environment* 68, 297–314.
843 <https://doi.org/10.1016/j.atmosenv.2012.11.027>
- 844 Tan, Z., Lu, K., Jiang, M., Su, R., Dong, H., Zeng, L., Xie, S., Tan, Q., Zhang, Y., 2018.
845 Exploring ozone pollution in Chengdu, southwestern China: A case study from
846 radical chemistry to O₃-VOC-NO_x sensitivity. *Science of The Total*
847 *Environment* 636, 775–786. <https://doi.org/10.1016/j.scitotenv.2018.04.286>
- 848 Tonnesen, G.S., Dennis, R.L., 2000. Analysis of radical propagation efficiency to assess
849 ozone sensitivity to hydrocarbons and NO_x: 2. Long-lived species as indicators
850 of ozone concentration sensitivity. *Journal of Geophysical Research:*
851 *Atmospheres* 105, 9227–9241. <https://doi.org/10.1029/1999JD900372>
- 852 Vermeuel, M.P., Novak, G.A., Alwe, H.D., Hughes, D.D., Kaleel, R., Dickens, A.F.,
853 Kenski, D., Czarnetzki, A.C., Stone, E.A., Stanier, C.O., Pierce, R.B., Millet,
854 D.B., Bertram, T.H., 2019. Sensitivity of Ozone Production to NO_x and VOC
855 Along the Lake Michigan Coastline. *Journal of Geophysical Research:*
856 *Atmospheres* 124, 10989–11006. <https://doi.org/10.1029/2019JD030842>



- 857 Wang, C., Huang, X.-F., Han, Y., Zhu, B., He, L.-Y., 2017. Sources and Potential
858 Photochemical Roles of Formaldehyde in an Urban Atmosphere in South China.
859 *Journal of Geophysical Research: Atmospheres* 122, 11,934–11,947.
860 <https://doi.org/10.1002/2017JD027266>
- 861 Wang, Y., Guo, H., Zou, S., Lyu, X., Ling, Z., Cheng, H., Zeren, Y., 2018. Surface O₃
862 photochemistry over the South China Sea: Application of a near-explicit
863 chemical mechanism box model. *Environmental Pollution* 234, 155–166.
864 <https://doi.org/10.1016/j.envpol.2017.11.001>
- 865 Xue, L., Gu, R., Wang, T., Wang, X., Saunders, S., Blake, D., Louie, P.K.K., Luk,
866 C.W.Y., Simpson, I., Xu, Z., Wang, Z., Gao, Y., Lee, S., Mellouki, A., Wang, W.,
867 2016. Oxidative capacity and radical chemistry in the polluted atmosphere of
868 Hong Kong and Pearl River Delta region: analysis of a severe photochemical
869 smog episode. *Atmospheric Chemistry and Physics* 16, 9891–9903.
870 <https://doi.org/10.5194/acp-16-9891-2016>
- 871 Xue, L.K., Wang, T., Gao, J., Ding, A.J., Zhou, X.H., Blake, D.R., Wang, X.F., Saunders,
872 S.M., Fan, S.J., Zuo, H.C., Zhang, Q.Z., Wang, W.X., 2014. Ground-level ozone
873 in four Chinese cities: precursors, regional transport and heterogeneous
874 processes. *Atmospheric Chemistry and Physics* 14, 13175–13188.
875 <https://doi.org/10.5194/acp-14-13175-2014>
- 876 Xue, L.K., Wang, T., Guo, H., Blake, D.R., Tang, J., Zhang, X.C., Saunders, S.M., Wang,
877 W.X., 2013. Sources and photochemistry of volatile organic compounds in the
878 remote atmosphere of western China: results from the Mt. Waliguan
879 Observatory. *Atmospheric Chemistry and Physics* 13, 8551–8567.
880 <https://doi.org/10.5194/acp-13-8551-2013>
- 881 Yang, X., Xue, L., Wang, T., Wang, X., Gao, J., Lee, S., Blake, D.R., Chai, F., Wang,
882 W., 2018. Observations and Explicit Modeling of Summertime Carbonyl
883 Formation in Beijing: Identification of Key Precursor Species and Their Impact
884 on Atmospheric Oxidation Chemistry. *Journal of Geophysical Research:*
885 *Atmospheres* 123, 1426–1440. <https://doi.org/10.1002/2017JD027403>
- 886 Yang, X., Xue, L., Yao, L., Li, Q., Wen, L., Zhu, Y., Chen, T., Wang, X., Yang, L., Wang,
887 T., Lee, S., Chen, J., Wang, W., 2017. Carbonyl compounds at Mount Tai in the
888 North China Plain: Characteristics, sources, and effects on ozone formation.
889 *Atmospheric Research* 196, 53–61.
890 <https://doi.org/10.1016/j.atmosres.2017.06.005>
- 891 Yuan, B., Chen, W., Shao, M., Wang, M., Lu, S., Wang, Bin, Liu, Y., Chang, C.-C.,
892 Wang, Boguang, 2012. Measurements of ambient hydrocarbons and carbonyls
893 in the Pearl River Delta (PRD), China. *Atmospheric Research, Remote Sensing*
894 *of Clouds and Aerosols: Techniques and Applications - Atmospheric Research*
895 116, 93–104. <https://doi.org/10.1016/j.atmosres.2012.03.006>
- 896 Zhang, X., Chen, Z.M., Zhao, Y., 2010. Laboratory simulation for the aqueous OH-
897 oxidation of methyl vinyl ketone and methacrolein: significance to the in-cloud
898 SOA production. *Atmospheric Chemistry and Physics* 10, 9551–9561.
899 <https://doi.org/10.5194/acp-10-9551-2010>
- 900 Zhang, X., Wu, Z., He, Z., Zhong, X., Bi, F., Li, Y., Gao, R., Li, H., Wang, W., 2022.



901 Spatiotemporal patterns and ozone sensitivity of gaseous carbonyls at eleven
902 urban sites in southeastern China. *Science of The Total Environment* 824,
903 153719. <https://doi.org/10.1016/j.scitotenv.2022.153719>
904 Zhang, Y., Wang, X., Wen, S., Herrmann, H., Yang, W., Huang, X., Zhang, Z., Huang,
905 Z., He, Q., George, C., 2016. On-road vehicle emissions of glyoxal and
906 methylglyoxal from tunnel tests in urban Guangzhou, China. *Atmospheric*
907 *Environment* 127, 55–60. <https://doi.org/10.1016/j.atmosenv.2015.12.017>
908 Zhang, Z., Zhang, Y., Wang, X., Lü, S., Huang, Z., Huang, X., Yang, W., Wang, Y.,
909 Zhang, Q., 2016. Spatiotemporal patterns and source implications of aromatic
910 hydrocarbons at six rural sites across China’s developed coastal regions. *Journal*
911 *of Geophysical Research: Atmospheres* 121, 6669–6687.
912 <https://doi.org/10.1002/2016JD025115>
913 Zhou, Z., Tan, Q., Deng, Y., Lu, C., Song, D., Zhou, X., Zhang, X., Jiang, X., 2021.
914 Source profiles and reactivity of volatile organic compounds from
915 anthropogenic sources of a megacity in southwest China. *Science of The Total*
916 *Environment* 790, 148149. <https://doi.org/10.1016/j.scitotenv.2021.148149>
917